TELKOMNIKA Telecommunication Computing Electronics and Control
Vol. 23, No. 6, December 2025, pp. 1439~1448
ISSN: 1693-6930, DOI: 10.12928/TELKOMNIKA.v23i6.27047

Reconfigurable ultra-wideband hexagonal antenna with two notched-band features for wireless applications

Khaled B. Suleiman[1], Akrem Asmeida[2], Shipun Anuar Hamzah[3], Mohd Shamian bin Zainal[4]
[1]Department of Electrical and Electronic Engineering, Faculty of Engineering, Azzaytuna University, Tarhuna, Libya
[2]Department of Networking, College of Computer Technology Zawiya, Al-Zawiya, Libya
[3]Department of Electrical and Electronic Engineering, Faculty of Engineering, UTHM University, Batu Pahat, Johor, Malaysia
[4]Department of Electrical Engineering Technology, Faculty of Engineering Technology, UTHM University, Muar, Johor, Malaysia

Article Info

Article history:

Received Mar 3, 2025
Revised Sep 28, 2025
Accepted Oct 19, 2025

Keywords:

CST Microwave Studio
Frequency reconfigurable
Lumped element
Notch filters
Ultra-wideband

ABSTRACT

Owing to the demand for frequency agility, a switchable ultra-wideband (UWB) hexagonal antenna was developed in this study. The proposed antenna features two notch filters introduced by two U-shaped slots on the patch to reduce interference from other wireless networks by rejecting the unique frequency bands. In addition, the proposed antenna comprises a hexagonal radiator attached to a feeding 50 Ω standard microstrip line. To fabricate the antenna prototype, a substrate (Rogers RT/Duroid 5880) with loss tangent and relative permittivity values of 0.0009, and 2.2, respectively, was used. Frequency and pattern reconfigurability were achieved by changing the electrical equivalent circuit of two positive-intrinsic-negative (PIN) diodes sandwiched within two U-shaped slots. The evaluation confirmed that the antenna operated within the D1&D2-ON configuration across the entire UWB range while, effectively filtering the wireless body area network (WBAN) (6.10–6.56 GHz) and radar application (9.16–10.79 GHz) bands when both diodes were OFF. The radiation efficiency and gain reached values of 92.9 % and 7.5 dB, respectively. The proposed design offers a robust performance with enhanced interference rejection. This makes it suitable for modern cognitive radio systems.

Corresponding Author:

Khaled B. Suleiman
Department of Electrical and Electronic Engineering, Faculty of Engineering, Azzaytuna University
Tarhuna, Libya
Email: k.suleiman@azu.edu.ly

1. INTRODUCTION

Recent advancements in wireless communication are driving an increasing need for antennas with higher bandwidth to support a range of high-performance applications [1], [2]. Ultra-wideband (UWB) has piqued researchers' interest because of its several advantages , including low cost, extra low spectral power density, improved data resolution, low complexity, and high data transmission rate with relatively low interference [3]-[7]. Following the designation of the 3.1–10 GHz frequency band for UWB communication by the Federal Communications Commission (FCC) in 2002, it has drawn the attention of many researchers and academics [8], [9]. Nonetheless, the implementation of UWB systems has faced significant challenges, one of which is the interference of the UWB technology with other narrowband systems such as worldwide interoperability for microwave access (WiMAX) 3.3 to 3.7 GHz, HiperLAN2 5.47 to 5.725 GHz, wireless local area network (WLAN) 5.15 to 5.35 GHz, 5.725 to 5.825 GHz, and X band satellite frequency system 7.9 to 8.4 GHz [10]. Unwanted in-band or out-of-band signals will impair the UWB receiver's functionality, and one popular and effective way to address this problem is to add a narrowband band-stop filter to the antenna's output. However, this approach causes issues such as impedance matching and increases the system's overall cost and complexity [11].

As a result, researchers have employed techniques such as metamaterials, defective ground structure (DGS), and etching slots in the patch to obtain notch band features [12]. It is well known that most antennas and filters are designed independently, and the majority of UWB antennas concentrate on band-notched functions, innovative structures, and reduction technologies [13]. Numerous techniques, including ground [14], [15], radiator grooves [16], feed line [17], and adding strips to the radiator [18], have been used to generate notch bands in the UWB spectrum.

The notched bands, however, are immovable after these designs are produced; in some cases, this limitation becomes problematic because the notch bands are unnecessary when there is no interference from the narrow band systems. As a solution, the frequency reconfigurable antenna is likely the most feasible option for switching its functioning to the required frequency [19]. Reconfigurable antennas have thus been divided into three groups: polarization, pattern, and frequency reconfigurable [20]. To adapt to changing operational requirements, a reconfigurable antenna's main working concept involves modifying one or more of its operational properties electrically, mechanically, or structurally using smart materials. The commonest RF switches used these days for reconfigurable antenna design include positive-intrinsic-negative (PIN) diodes, field-effect transistors (FETs), radiofrequency micro-electromechanical system (RFMEMS) switches, and micro-electromechanical system (MEMS) switches [21]-[25].

In this study, a reconfigurable UWB antenna with notched band characteristics is designed and modeled for wireless systems. Initially, the proposed antenna was optimized to cover the entire UWB frequency range and to achieve improved return loss (RL) performance. Subsequently, two U-shaped slots are etched into the antenna to introduce the desired band-notch characteristics. Finally, two PIN diodes were integrated into the U-slots, enabling reconfigurability in the design. Three operational modes are achieved by switching the PIN diodes between their ON and OFF states.

According to Table 1, it is evident that the proposed antenna exceeds existing the designs in several key aspects. It attains a wide UWB bandwidth of 11.29 GHz, significantly exceeding the bandwidths of 9.8 GHz, 9.9 GHz, 9.4, and 8.56 GHz found in the literature [5], [26]-[28]. In terms of dimensions, the suggested antenna is more compact than mentioned in [5]. Achieving a radiation efficiency of 92.2%, the proposed design notably surpasses the 80% and 85% efficiencies reported in studies [5], [28].With a significant gain of 7 dB, the suggested antenna outperforms the gains of 5.3 dB, 4.6 dB, 6 dB, and 4 dB described in references[5], [26]-[28], respectively. Overall, the comprehensive analysis highlights the significant improvements and improved performance features of the suggested antenna design, demonstrating its potential to establish a new benchmark in antenna technology.

Table 1. Comparison between various frequency reconfigurable antennas

Ref.	Size (mm2)	Notch bands (GHz)	Bandwidth (GHz)	No. of operating states	Switching technique	Gain (dB)	Radiation efficiency %
[5]	40×40	3.1–3.5, 3.64–4, 4.58–4.74, 5.14–5.3	2.2–12	16	4 PIN diodes	5.3	80%
[26]	33×34	2, 3.5, 5.8	1.4–11.3	4	Using specific parameters	3.6–4.6	NG*
[27]	26×36.6	3.6, 5.6–7.7	3.1–12.5	4	1 Varactor diode	6	NG*
[28]	34.9×31	1.58–2.12, 2.24–2.68, 3.08–3.78	1.98–10.5	8	3 Varactor diodes	3-4	85%
This work	43.5×26	6.08–6.50, 9.16–10.79	4.75–16.04	3	2 PIN diodes	7	92.2

NG* = not given

2. RECONFIGURABLE ANTENNA DESIGN METHODOLOGY

The hexagonal reconfigurable dual notched-band UWB antenna built in this work is depicted in Figures 1(a) and (b). The antenna geometry was created from a Rogers RT/Duroid 5880 substrate, 1.58 mm thickness, 2.2 relative permittivity (εr), and 0.0009 loss tangent ($tan\ \delta$). This material was chosen for its low dielectric constant, which decreases the signal latency, improves the impedance matching, and reduces the surface wave losses, resulting in a higher radiation efficiency. Furthermore, its extraordinarily low loss tangent minimizes the signal attenuation, enhancing the antenna gain and overall performance. Compared to the widely used rectangular and circular geometries, the suggested hexagonal shape offers improved compactness and inherent geometry characteristics. Its symmetrical construction additionally decreases the edge diffraction, potentially improving the bandwidth and radiation performance [1], [3]. The recommended antenna's overall dimensions are 43.5×26×1.6 mm².

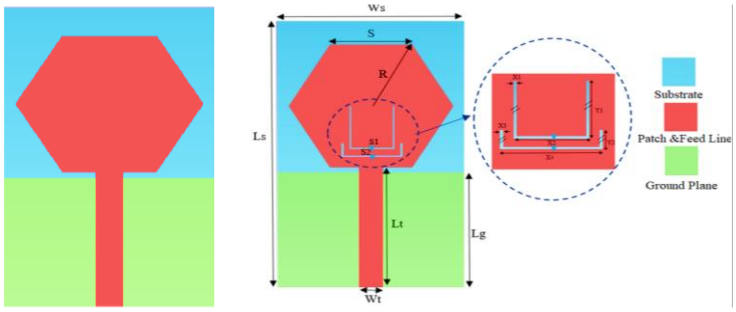

(a) (b)

Figure 1. UWB antenna geometry: (a) hexagonal patch with partial ground and (b) proposed reconfigurable antenna structure

To improve the impedance matching between the 50 Ω coaxial cable attached to the subminiature version A (SMA) connector and the high impedance at the patch edge, a microstrip feedline was used to feed the proposed antenna. To improve and move from the conventional narrow band to a wider bandwidth, the modified ground plane technique was employed. Having two U-shaped slots on the radiating patch results in a frequency-notched feature. At the optimal position, two PIN diode switches are integrated at the two U-shaped slots for pattern reconfiguration and surface current concentration redistribution. The proposed reconfigurable antenna was designed and modeled using the computer simulation technology (CST) 2020 software. Nevertheless, the spectrum analyzer was used to test the prototype antenna after it was physically implemented. The analogous circuits for using the PIN diodes in both the ON and OFF states are displayed in Figure 2, while the physical attributes and essential components of the tuned antenna are described in Table 2. The side length and the effective radius of the hexagonal patch's circular patch can be calculated as follows to accomplish a specific frequency operation [1].

$$a_e = a\left(1 - \frac{2h}{\pi a \mathcal{E}_r}\left(\ln\frac{\pi}{2h} + 1.7726\right)\right)^{\frac{1}{2}} \quad (1)$$

$$\pi a_e^2 = \left(\frac{3\sqrt{3}}{2}\right)s^2 \quad (2)$$

where:
a = circular patch antenna's actual radius
a_e = circular patch antenna's effective radius
h = substrate height
εr = substrate relative permittivity
S = sides of a regular hexagonal patch antenna

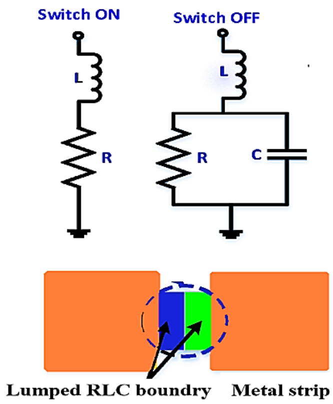

Figure 2. Equivalent circuit of the PIN diode model [12]

Table 2. The proposed antenna design parameters

Parameter	Dimension (mm)
Radius (R) of the hexagon patch	11.50
Length (S) of the hexagon patch segment	11.50
Transmission line length (Lt)	19.59
Transmission line width (Wt)	3.4
Length (Ls) Substrate	43.5
Width (Ws) Substrate	26
Ground plane length (Lg)	18.80
1st U slot dimensions ($X1$), ($Y1$), ($X2$)	0.25, 7, 6.25
2nd U slot 2 dimensions ($X3$), ($Y2$), ($X4$)	0.25, 2.25, 8.50

3. OUTCOMES AND DISCUSSIONS

This section provides an explanation and a detailed discussion of the study findings for the suggested UWB reconfigurable antenna.

3.1. Return loss (S_{11}) of the UWB antenna

An effective antenna should have a RL value of -10 dB. Taking into account that 90 % of the signal is transmitted and only 10 % is reflected, this threshold is chosen. To obtain a UWB response, the proposed antenna's ground plane length was parametrically analyzed. Figure 3(a) illustrates the influence of the different ground plane lengths (Lg) on the RL. The parametric Analysis identifies 18.80 mm as the ideal ground plane length, ensuring good impedance matching and a consistent UWB response from 4.75 to 16.04 GHz with minimum resonance shifting. The RLs for the conventional and final designs are contrasted in Figure 3(b).

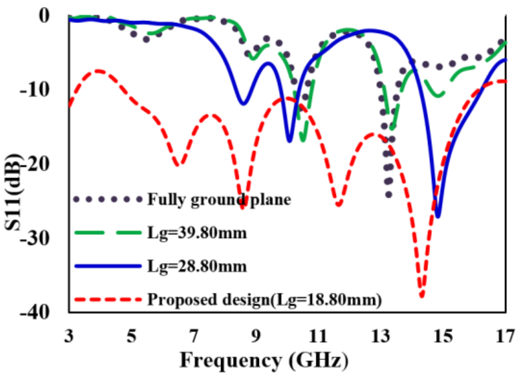

(a)

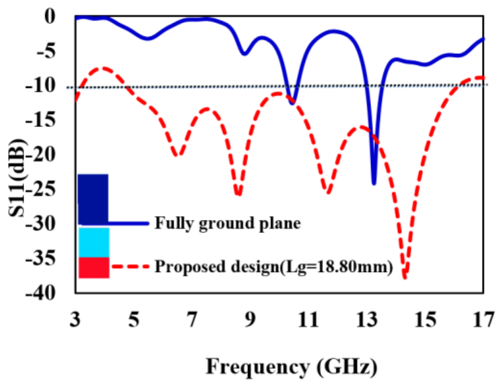

(b)

Figure 3. Parametric study of ground plane: (a) reflection coefficient response with different Lg and (b) S_{11} reaction both before and after utilizing a partial ground plane

3.2. Return loss of the proposed reconfigurable antenna

An analogous lumped resistor-inductor-capacitor (RLC) circuit was used to represent the PIN diodes. The resonant frequency changes when the PIN diode is switched because it alters the current distribution in the defective ground plane. Figure 4(a) demonstrates the aggregate S_{11} values for each of the three potential switching configurations. The operating modes of the proposed reconfigurable dual-band notch conditions are described in Table 3. The mode of the targeted notched band of wireless body area network (WBAN) (6.10-6.56 GHz) and radar applications (9.16–10.79 GHz) are controlled by the ON and OFF states of the PIN diodes. Thus, the simulated RL results are satisfactory at different reconfigurable frequencies.

3.3. Voltage standing wave ratio (VSWR) of the proposed antenna

The VSWR indicates the antenna's impedance matching capabilities; a practical value of less than 2 is required, while the ideal value of VSWR is 1. Figure 4(b) clarifies the notched features of the proposed antenna. It was found that the single band-notched antenna (mode B) could function with a VSWR of >2 from 4.81 to 16.04 GHz, except for one stopband from 6.10 to 6.56 GHz. Two stopbands, however, are observed when both switches were in the OFF position (scenario C): WBAN (6.10–6.56 GHz) and radar applications (9.16–10.79 GHz). To verify the design and simulation outcomes, the antenna is designed as shown in Figure 5. Due to the lack of diodes in the utilized lab, three different designs of the antenna were made.

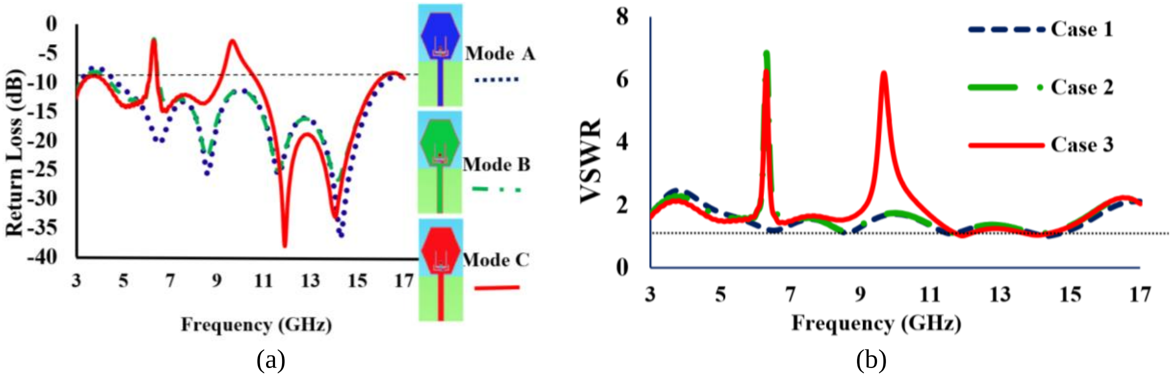

Figure 4. Performance characteristics of the proposed antenna: (a) simulated S_{11} and (b) VSWR simulation of the proposed antenna

Table 3. Operating states of the proposed reconfigurable UWB antenna

Mode	Diode states D1	D2	Operating band (GHz)	Bandwidth (GHz)	No. of band	Resonance frequency (GHz)	RL (dB)	Notched band (GHz)
A	ON	ON	4.81–16.04	11.2	UWB	6.50, 8.51, 11.5, 14.52	20.52, 24.19, 25.77, 36.33	-
B	OFF	ON	4.16–6.07 6.60–15.82	1.91 9.82	2	11.5, 13.5	37, 32	6.10–6.56
C	OFF	OFF	4.16–6.07 6.53–9.20 10.80–15.82	1.91 2.67 5.02	3	8.5, 11.3, 13.5	24,26,27	6.08–6.50 9.16–10.79

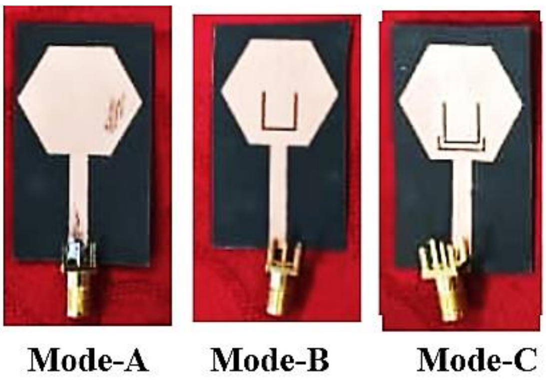

Figure 5. The proposed antenna's prototype

3.4. Effect of PIN diodes status on the proposed antennas' surface current distribution

Figures 6(a) to 6(d) show the surface currents for modes 1–3 in detail and illustrate the reconfigurable antenna operation mechanism. For instance, the surface current distributions of Case 1 for all resonant frequencies (6.5, 8.5, 11.5, and 14.5 GHz) are concentrated near the feeding line and on the edge of the hexagon radiating element. As seen, the antenna's current distribution is controlled by turning the diodes ON and OFF; this alters the resonating frequency and the current flowing over the antenna's surface. The corner of the U slots exhibits the largest current distribution for both modes (A and B) when one or both PIN diodes are OFF.

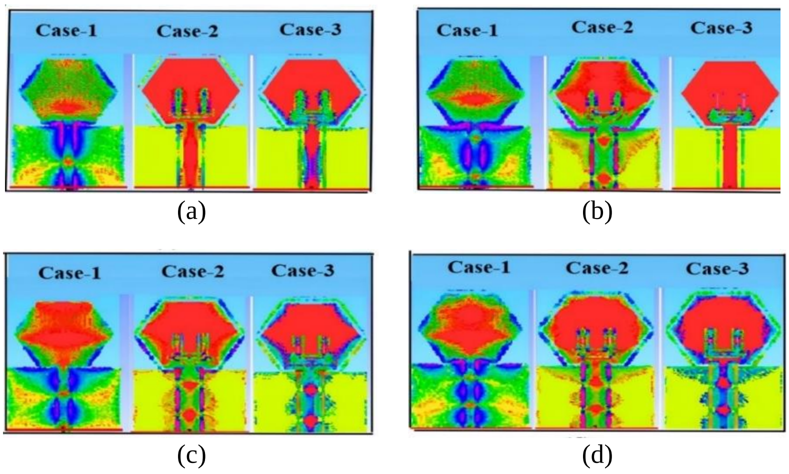

Figure 6. Surface current distribution of all cases at: (a) 6.5 GHz, (b) 8.5 GHz, (c) 11.5 GHz, and (d) 14.5 GHz

3.5. Realized gain and radiation efficiency

The proposed antenna's simulated gain with and without notch filters (two switching configurations) is contrasted in Figure 7(a). As seen, except for the two stopbands, the simulated peak gain ranges from 2.5 to 7.5 dBi throughout the whole UWB frequency band. The proposed antenna recorded 92.2% efficiency for the 6.5 to 117 GHz frequency range, as depicted in Figure 7(b). Hence, the antenna efficiency variation is suitable for UWB terminals in wireless applications.

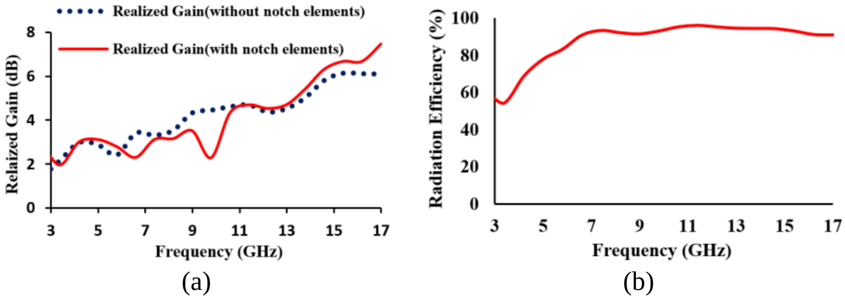

Figure 7. Analysis of the designed antenna parameters: (a) simulated gain performance of the antenna with/without notch filters and (b) efficiency-frequency curve of the designed antenna

3.6. Comparison of the measured and simulated RL of the reconfigurable antenna

The actual (measured) and simulated RL of the proposed antenna are contrasted in Table 4. When both D1 and D2 are activated, the simulated operating band is recognized as 4.81 GHz to 16.04 GHz; nevertheless, the measured band is 6.20 GHz to 12.10 GHz. The observed reflection coefficients show a narrower range. Additionally, a suppressed band is detected between 5.8 GHz and 6.1 GHz, which indicates slight differences due to losses experienced during the actual implementation. When both D1 and D2 are deactivated, the simulated results show multiple bands: 4.16–6.07 GHz, 6.53–9.20 GHz, and 10.80–15.82 GHz. In the corresponding measured findings, an enlarged filtered band appears at 11.10–16.30 GHz; additional bands are also seen at 4.82–5.81 GHz and 10.11–11.50 GHz. These results indicate improved operating efficiency at higher frequencies, yet possibly a drop-in performance at lower frequencies.

Functioning with D1-OFF and D2-ON mixed diode states: the 4.16–6.07 GHz and 6.60–15.82 GHz ranges are observed to be the simulated functioning bands. The disparity between the simulated and measured RL, particularly the frequency shifts, is most likely caused by the fabrication tolerances, substrate imperfections, and connector or soldering losses. To mitigate these impacts, more precise fabrication, improved soldering procedures, and closer component matching are suggested. Furthermore, incorporating varactors or surface mount technology (SMT) soldering allows tuning of notched bands, enhancing performance in dynamic wireless situations.

Table 4. The actual and simulated reflection coefficients of the proposed antenna

Diode status	Simulated results		Meas results	
	Operating band (GHz)	Filtered band (GHz)	Operating band (GHz)	Filtered band (GHz)
D1&D2-ON	4.81–16.04	-	6.20–12.10	5.8–6.1
D1&D2-OFF	4.16–6.07 6.53–9.20 10.80–15.82	6.08–6.50 9.16–10.79	4.82–5.81 10.11–11.50	5.09–10.09 11.10–16.30
D1-OFF&D2-ON	4.16–6.07 6.60–15.82	6.10–6.56	5.10–5.80 7.90–11.80	5.83–7.95 11.81–16.40

3.7. Radiation patterns at resonance frequencies

The three antenna modes (Modes 1, 2, 3) exhibited linearly polarized radiation patterns at the 6.5, 8.5, 11.5, and 14.5 GHz resonant frequencies (these patterns are depicted in Figures 8(a) to (d). Two patterns of radiation are displayed in each polar plot: the blue dashed line indicates radiation at ɵ=90° (H-plane), while the red solid line indicates radiation at ɵ=0° (E-plane). At lower frequencies, the radiation patterns are relatively simple, particularly in Mode-1 (D1&D2-ON), where symmetry is evident at 6.5 GHz. As the frequency increases, the patterns develop additional complexity.

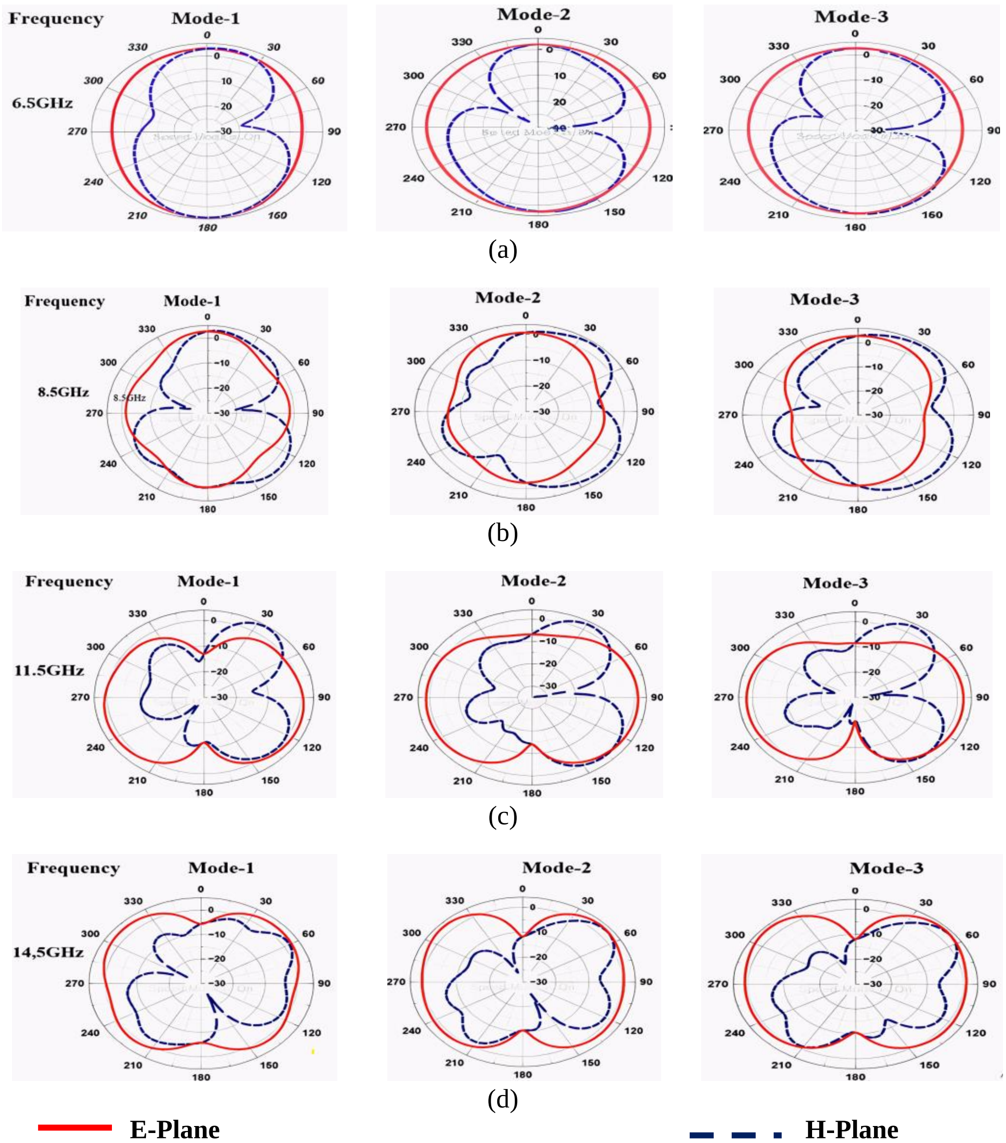

Figure 8. The antenna's far-field radiation pattern (E- and H-planes) for the studied modes at: (a) 6.5 GHz, (b) 8.5 GHz, (c) 11.5 GHz, and (d) 14.5 GHz

To illustrate, among the three scenarios, the radiation patterns show the most complexity at the highest frequency, 14.5 GHz. Specifically, at ɵ=0°, Mode-1 exhibits a symmetrical, multi-lobed pattern, while at ɵ=90°, Mode-2 (D1 OFF and D2 ON) shows a directional shift with more obviously expanded lobes. The lobes in Mode-3, in contrast, are diffuse and wide, with complicated and irregular forms in both directions, likely due to the switching mode of the two PIN diodes in this case. The radiation pattern is reconfigurable.

4. CONCLUSION

The development and evaluation of a reconfigurable UWB hexagonal antenna with two notched band characteristics are detailed in this work. Using the etched slots (two U slots) approach, notch band features were obtained. For pattern reconfiguration and surface current concentration redistribution, two PIN diodes (D1&D2) switches are sandwiched in the two U-shaped slots at the optimal positions. The antenna successfully covered the full UWB range (4.75–16.04 GHz) in the ON state while selectively rejecting interference from the WBAN and radar frequency bands in the off state. The obtained results confirmed a VSWR below 2, a high radiation efficiency of 92.9%, and a peak gain of 7.5dB. These findings indicate that the proposed antenna not only delivers superior performance but also improves interference suppression, making it a promising option for reconfigurable UWB systems in future wireless applications. Besides, the designed element could be a precursor to the development of a multiple-input multiple-output (MIMO) antenna for subsequent studies to enhance the system capacity and transmission rate.

ACKNOWLEDGEMENTS

The authors of this research paper would like to thank "Azzaytuna University, University Tun Hussein Onn Malaysia (UTHM) Office for Research, Innovation, Commercialization and Consultancy Management (ORICC)," and the internship students from the Islamic University of Medina for their contributions. Special thanks to Mr. Basam Mohamed Alawaji, Mr. Mustafa Kamil Eltayeb, and Mr. Albaraa Shouki Ebad for their support during this research work.

FUNDING INFORMATION

This work was not supported by a specific grant; therefore, no grant number is available. The publication fees will be covered by Azzaytuna University after the article is published.

AUTHOR CONTRIBUTIONS STATEMENT

This journal uses the Contributor Roles Taxonomy (CRediT) to recognize individual author contributions, reduce authorship disputes, and facilitate collaboration.

Name of Author	C	M	So	Va	Fo	I	R	D	O	E	Vi	Su	P	Fu
Khaled B. Suleiman	✓	✓	✓	✓	✓	✓	✓	✓	✓	✓			✓	✓
Akrem Asmeida	✓		✓	✓		✓	✓	✓	✓	✓	✓			✓
Shipun Anuar Hamzah	✓		✓	✓	✓		✓	✓		✓	✓	✓	✓	
Mohd Shamian bin Zainal		✓		✓			✓			✓		✓	✓	

C : **C**onceptualization
M : **M**ethodology
So : **So**ftware
Va : **Va**lidation
Fo : **Fo**rmal analysis
I : **I**nvestigation
R : **R**esources
D : **D**ata Curation
O : Writing - **O**riginal Draft
E : Writing - Review & **E**diting
Vi : **Vi**sualization
Su : **Su**pervision
P : **P**roject administration
Fu : **Fu**nding acquisition

CONFLICT OF INTEREST

There is no existing conflict of interest regarding the publication of this study.

DATA AVAILABILITY

All the data related to this study have been included in this article.

REFERENCES

[1] N. A. Jan *et al.*, "Design of a compact monopole antenna for UWB applications," *Computers, Materials and Continua*, vol. 66, no. 1, pp. 35–44, 2021, doi: 10.32604/cmc.2020.012800.

[2] P. Pannu, "Highly compact UWB-MIMO antenna with sharp multi-stop band characteristics," *Eurasip Journal on Wireless Communications and Networking*, vol. 2024, no. 1, 2024, doi: 10.1186/s13638-024-02369-1.

[3] Z. Yu *et al.*, "A flexible multi-band antenna with a spider web-like structure for 4G/5G/GPS/WIMAX/WLAN Applications," *Electronics (Switzerland)*, vol. 14, no. 2, 2025, doi: 10.3390/electronics14020253.

[4] A. Zaidi *et al.*, "A Low Profile Ultra-wideband antenna with reconfigurable notch band characteristics for smart electronic systems," *Micromachines*, vol. 13, no. 11, 2022, doi: 10.3390/mi13111803.

[5] R. B. Sadineni, K. Srinivasa Rao, T. Sushma, P. V. K. Kanth, V. Ramakoteswara Rao, and D. P. Gowda, "Design of ultra-wideband antenna with quadruple band notch reconfigurability," *Progress In Electromagnetics Research C*, vol. 144, pp. 23–31, 2024, doi: 10.2528/PIERC24032302.

[6] P. P. Shome and T. Khan, "Switchable triple band-notched UWB antenna modelling for interference rejection from dual WiMAX bands and satellite C-band service," *Journal of Electromagnetic Waves and Applications*, vol. 34, no. 15, pp. 2010–2029, 2020, doi: 10.1080/09205071.2020.1806115.

[7] S. Park and K. Y. Jung, "Novel compact UWB planar monopole antenna using a ribbon-shaped slot," *IEEE Access*, vol. 10, pp. 61951–61959, 2022, doi: 10.1109/ACCESS.2022.3182443.

[8] M. M. Fakharian, "A compact UWB antenna with dynamically switchable band-notched characteristic using broadband rectenna and DC-DC booster," *International Journal of Microwave and Wireless Technologies*, vol. 13, no. 10, pp. 1086–1095, 2021, doi: 10.1017/S1759078721000027.

[9] K. B. Suleiman, A. A. Albishti, and S. A. Hamzah, "Design and analysis of dipole ultra wide band antenna for wireless applications," in *2022 IEEE 2nd International Maghreb Meeting of the Conference on Sciences and Techniques of Automatic Control and Computer Engineering (MI-STA)*, IEEE, May 2022, pp. 427–430, doi: 10.1109/MI-STA54861.2022.9837683.

[10] H. Lin, Z. Lu, Z. Wang, and W. Mu, "A Compact UWB Monopole Antenna with Triple Band Notches," *Micromachines*, vol. 14, no. 3, 2023, doi: 10.3390/mi14030518.

[11] S. Agrawal, Z. Wani, and M. S. Parihar, "Patch loaded slot antenna for super wideband applications with dual-band notch characteristic," *Wireless Personal Communications*, vol. 123, no. 4, pp. 3051–3064, 2022, doi: 10.1007/s11277-021-09276-4.

[12] O. P. Kumar, P. Kumar, T. Ali, P. Kumar, and S. B. K, "A quadruple notch UWB antenna with decagonal radiator and sierpinski square fractal slots," *Journal of Sensor and Actuator Networks*, vol. 12, no. 2, 2023, doi: 10.3390/jsan12020024.

[13] S. Mukherjee, A. Roy, S. Maity, T. Tewary, P. P. Sarkar, and S. Bhunia, "Design of dual band-notched UWB hexagonal printed microstrip antenna," *International Journal of Microwave and Wireless Technologies*, vol. 15, no. 3, pp. 526–534, 2023, doi: 10.1017/S1759078722000447.

[14] Z. Wang, X. Liu, N. Rasool, Z. Tang, and F. Chen, "Dual band-notched ultra-wideband antenna with T-shape stub," *Electronics Letters*, vol. 58, no. 20, pp. 747–749, 2022, doi: 10.1049/ell2.12602.

[15] P. Muthusamy, S. Nallapaneni, K. C. Perumalla, and B. Punna, "Band notch characteristics reconfigurable UWB leaf shape monopole antenna," *International Journal of Electronics and Telecommunications*, vol. 68, no. 2, pp. 223–228, 2022, doi: 10.24425-ijet.2022.139871/958.

[16] N. Taher, A. Zakriti, N. A. Touhami, and F. Rahmani, "Circular ring UWB antenna with reconfigurable notch band at WLAN/sub 6 GHz 5G mobile communication," *Microsystem Technologies*, vol. 28, no. 4, pp. 965–972, 2022, doi: 10.1007/s00542-021-05246-9.

[17] K. Kaur, A. Kumar, and N. Sharma, "A novel design of ultra-wideband CPW-fed printed monopole antenna for Wi-MAX, WLAN and X-band rejection characteristics," *Analog Integrated Circuits and Signal Processing*, vol. 114, no. 1, pp. 143–157, 2023, doi: 10.1007/s10470-022-02132-w.

[18] K. Shaik and V. Kumar, "Compact triple band notched UWB MIMO antenna with integrated GSM," *International Journal of Communication Systems*, vol. 37, no. 6, 2024, doi: 10.1002/dac.5708.

[19] J. Su, Y. Li, X. Chen, G. Han, and W. Zhang, "A compact triple band-notched quasi-self-complementary UWB MIMO antenna decoupled by SRRs," *International Journal of Microwave and Wireless Technologies*, vol. 15, no. 7, pp. 1251–1261, 2023, doi: 10.1017/S1759078722001325.

[20] S. Subbaraj and S. B. Thomas, "Reconfigurable antennas and their practical applications—a review," *Radio Science*, vol. 58, no. 9, Sep. 2023, doi: 10.1029/2023RS007656.

[21] D. Zhou, H. Wang, L. Deng, L. L. Qiu, and S. Huang, "Metamaterial-based frequency reconfigurable microstrip antenna for wideband and improved gain performance," *International Journal of RF and Microwave Computer-Aided Engineering*, vol. 32, no. 2, 2022, doi: 10.1002/mmce.22988.

[22] K. B. Suleiman and A. A. Albishti, "Reconfigurable meander line dipole antenna based on two rectangular defected ground structure," *Telkomnika (Telecommunication Computing Electronics and Control)*, vol. 21, no. 6, pp. 1196–1203, 2023, doi: 10.12928/TELKOMNIKA.v21i6.25288.

[23] M. Donelli, J. Iannacci, and M. Manekiya, "A new concept of reconfigurable antenna structure based on an array of RF-MEMS switches," *Applied Sciences (Switzerland)*, vol. 14, no. 23, 2024, doi: 10.3390/app142310941.

[24] Z. Fang *et al.*, "Design of a 2-bit reconfigurable UWB planar antenna array for beam scanning application," *IEEE Open Journal of Antennas and Propagation*, vol. 4, pp. 91–96, 2023, doi: 10.1109/OJAP.2023.3234541.

[25] S. Nej, A. Ghosh, J. Kumar, and S. Das, "Ultra-wideband MIMO antenna with reconfigurable band notch characteristics and improved isolation," *AEU - International Journal of Electronics and Communications*, vol. 170, p. 154849, Oct. 2023, doi: 10.1016/j.aeue.2023.154849.

[26] A. Iqbal, A. Smida, N. K. Mallat, M. T. Islam, and S. Kim, "A compact UWB antenna with independently controllable notch bands," *Sensors*, vol. 19, no. 6, p. 1411, Mar. 2019, doi: 10.3390/s19061411.

[27] N. Moradi, F. Nazari, H. Aliakbarian, and F. A. Namin, "Compact ultrawideband monopole antenna with continuously tunable notch band characteristics," *Progress In Electromagnetics Research C*, vol. 118, pp. 71–81, 2022, doi: 10.2528/PIERC21120207.

[28] P. P. Shome, T. Khan, and R. H. Laskar, "CSRR-loaded UWB monopole antenna with electronically tunable triple band-notch characteristics for cognitive radio applications," *Microwave and Optical Technology Letters*, vol. 62, no. 9, pp. 2919–2929, 2020, doi: 10.1002/mop.32394.

BIOGRAPHIES OF AUTHORS

Khaled B. Suleiman received the B.Eng. degree in Electrical and Electronic Engineering from the University of Azzaytuna, Tarhuna, Libya, in 2008, and the Master's degree in Electronic Engineering from UTHM University, Malaysia, in 2015. He has been working as a lecturer in the Department of a Electrical and Electronic Engineering, University of Azzaytuna, Tarhuna, Libya since February 2016. At present, he is the coordinator of study and exams at the department. Additionally, he is a regular reviewer as well as a (PC) member of various IEEE conferences. His areas of research interest are harmonic suppression antenna, reconfigurable antenna, and smart antenna. system. He can be contacted at email: k.suleiman@azu.edu.ly.

Akrem Asmeida received his Ph.D. in Electrical Engineering from UTHM. He is a senior lecturer under the Department of Networking, College of Computer Technology Zawiya, Al-Zawiya, Libya. With extensive experience in high-frequency electronics, electromagnetic theory, and wireless communication systems, he has made significant contributions to the design, optimization, and analysis of advanced RF and microwave circuits. He can be contacted at email: asmeidaakrem@gmail.com.

Shipun Anuar Hamzah received Bachelor of Electrical Engineering from Universiti Teknologi Malaysia in 1998. He then received his M.Sc. in Communication and Computer from Universiti Kebangsaan Malaysia in 2000. He received his Ph.D. in Electrical Engineering from Universiti Teknologi Malaysia in 2014. His research interests are active antenna design, harmonic suppression antenna, and energy harvesting. He can be contacted at email: shipun@uthm.edu.my.

Mohd Shamian bin Zainal received B.Eng. (Electrical) and M.Eng. (Electrical) from Universiti Teknologi Malaysia (UTM) and Universiti Tun Hussein Onn Malaysia (UTHM) in 2000 and 2003, respectively. He obtained his Ph.D. in Electrical Engineering from Hokkaido University in 2010. His main areas of research interest are image processing, IoT, and big data. He can be contacted at email: shamian@uthm.edu.my.